# Multi-physics fem model of solar hybrid roads for energy harvesting performance evaluation in presence of semi-transparent or opaque pavement surface layer

Nicolas Le Touz, Jean Dumoulin, Jean Michel Piau

# MULTI-PHYSICS FEM MODEL OF SOLAR HYBRID ROADS FOR ENERGY HARVESTING PERFORMANCE EVALUATION IN PRESENCE OF SEMI-TRANSPARENT OR OPAQUE PAVEMENT SURFACE LAYER

**N. Le Touz,[1,*,3,*] J. Dumoulin,[1,3] J.-M. Piau[2]**

[1]IFSTTAR, COSYS-SII, Route de Bouaye, F-44344, Bouguenais, France
[2]ISFTTAR, MAST-LAMES, Route de Bouaye, F-44344, Bouguenais, France
[3]Inria, I4S Team, Campus de Beaulieu, F-35042 Rennes, France

## ABSTRACT

We present in this paper the concept of solar hybrid road and focus on the thermal performances of such system. Main differences between these multi-layer structures with traditional road structures come from the pavement surface, which can be opaque or semi-transparent and the porous sub-layer, submitted to fluid flow. These structures aim at collecting solar energy during the summer season, what helps also to prevent from a too high temperature and urban heat island effect. A finite element model is presented to couple thermal diffusion, hydraulic convection and radiative transfer. This numerical model allows to compute the temperature field for different weather conditions and also to evaluate the thermal performances of the system. Annual simulations are performed and a comparison between two surface layer solutions for different locations and climates is presented and discussed.

**KEY WORDS:** Computational methods, Energy efficiency, Multi-physics heat transfer, Solar hybrid road, Energy harvesting, Finite element model, Porous media

## 1. INTRODUCTION

As part of the energy transition, numerous studies have been led on renewable energy sources and energy management. Because of the increase of car traffic, road structures represent a large surface area that is still growing. These structures are in direct contact with the environment and subject to weather conditions. During summer conditions, road are submitted to heavy thermal load through solar and convective heat flux. The increase of temperature in the structure can provoke a degradation of mechanical performances entailing rutting and also contribute to the rise of urban heat island effect [5, 13]. During winter conditions, the surface temperature can decrease below 0°C what may entail black ice formation, and consequently safety and economic problems. Moreover, current practice consisting in salting the road entails environmental problems.

In order to avoid these problems, we propose to control the temperature of the road structure by a reversible system able to recover energy during the summer and bringing energy during cold periods. Traditional approaches to build such embedded energetic systems rely on a heat fluid flowing in tubes buried below the surface layer of the pavement [12, 13]. In this study, we present a solar hybrid road in which the fluid flows into a porous layer below the surface layer. To increase the ability of this hybrid road to harvest energy, a semi-transparent layer is used in order to favour solar radiation penetration in the structure.

*Corresponding N. Le Touz: nicolas.le-touz@ifsttar.fr

In this paper, computation of the temperature field in the structure with a multi-physics finite element model is first presented. This numerical model is then applied to calculate the energy harvesting during the summer period.

## 2. HYBRID SOLAR ROAD CONCEPT

This concept is based on a multilayer system for which the two layers closest to the surface have been modified, compared to traditional road structures. The multilayer system is shown in figure 1.

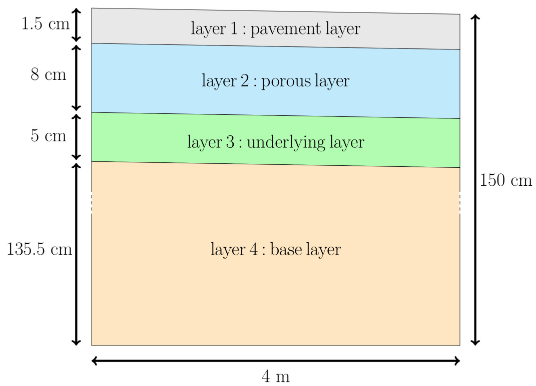


**Fig. 1** Sectional schematic view of modified road structure

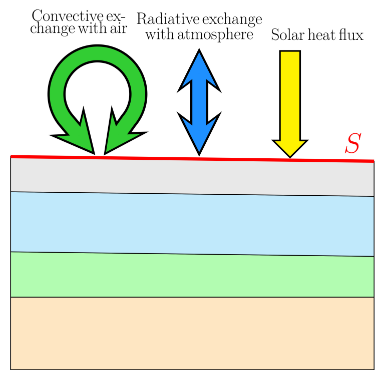


**Fig. 2** Interactions with the environment

Layer 1 is semi-transparent or opaque and waterproof. Layer 2 is porous: a fluid flows inside along the width of the road, with the effect of the imposed slope. Layer 3 and 4 are opaque and waterproof.

Thermal properties of materials considered, in this study, for numerical simulations are reported in table 1.

**Table 1** Thermal properties of layers and fluid (from [1, 7, 16])

| | layer 1 | layer 2 | layer 3 | layer 4 | fluid |
|---|---|---|---|---|---|
| $k$ [W.m$^{-1}$.K$^{-1}$] | 0.85 | 1.03 | 1.40 | 1.10 | 0.60 |
| $\rho$ [kg.m$^{-3}$] | 2700 | 2360 | 2620 | 2300 | 1000 |
| $C_p$ [J.kg$^{-1}$.K$^{-1}$] | 840 | 780 | 860 | 1000 | 4180 |

For optical properties, we take in a first approach properties of glass given by [15] and estimate them thanks to experimental mock-up [11]. They are reported in table 2.

**Table 2** Optical properties of the semi-transparent layer, from [15] for absorption coefficient $\kappa$

| $\lambda$ [µm] | $\lambda < 0.5$ | $0.5 \leq \lambda < 2.7$ | $2.7 \leq \lambda < 4.5$ | $4.5 \leq \lambda < 50$ | $\lambda \geq 50$ |
|---|---|---|---|---|---|
| $\kappa_\lambda$ [m$^{-1}$] | 0 | 10 | 1000 | 5000 | $+\infty$ |
| $\sigma_\lambda$ [m$^{-1}$] | 10 | 10 | 10 | 10 | 10 |

## 3. MULTI-PHYSIC NUMERICAL MODEL

Our model combining thermal diffusion, hydraulic convection and radiative transfer is presented hereafter

### 3.1 Thermal diffusion

The structure is submitted to convective exchange with the air, radiative exchange with the sky and solar radiation. Heat equation can be written as system 1. Depth of the structure is supposed to be large enough so that thermal exchanges can be neglected except at the surface $S$, shown in figure 2, where Robin boundary conditions are considered.

$$\begin{cases} \rho C_p \dfrac{\partial T}{\partial t} = \nabla \cdot [k \nabla T] + q \\ k \nabla T \cdot \vec{n} = \begin{cases} \Phi_s + h_{\text{conv}} (T_a - T) + h_{\text{rad}} \left( T_{\text{sky}} - T \right) & \text{on the surface} \\ 0 & \text{for other boundaries} \end{cases} \end{cases} \tag{1}$$

With $\rho$ the density, $C_p$ the heat capacity, $k$ the thermal conductivity, $h_{\text{conv}}$ the convective heat exchange coefficient, $h_{\text{rad}}$ the radiative exchange coefficient, $T_a$ the air temperature and $T_{\text{sky}}$ the sky temperature. The radiative exchange coefficient is given from sky and surface temperatures by $h_{\text{rad}} = \varepsilon\sigma(T_{\text{surf}}^2 + T_{\text{sky}}^2)(T_{\text{surf}} + T_{\text{sky}})$, where $\varepsilon$ is the surface emissivity and $\sigma$ the Stefan constant.

Finite element formulation of this problem has been widely studied, more information can be found in [4, 16].

## 3.2 Hydraulic convection

Two temperature fields are considered in the porous layer, for solid and fluid phases, respectively written $T$ and $T_f$. Equations on these temperature fields can be obtained from Navier-Stokes equations integrated over an elementary representative volume. With the hypothesis of a stationary flow, a low and uniform pore speed and a saturated porous layer [2, 14], we have:

$$(1 - \varphi) \rho_s C_{p,s} \frac{\partial T}{\partial t} = (1 - \varphi) \nabla \cdot [k \nabla T] + h (T_f - T) \tag{2}$$

$$\varphi \rho_f C_{p,f} \frac{\partial T_f}{\partial t} + \rho_f C_{p,f} \vec{u} \cdot \nabla T_f = \varphi \nabla \cdot [k_f \nabla T_f] + h (T - T_f) \tag{3}$$

Where $h$ is an exchange coefficient dependent of the pore and flow characteristics [14], $\vec{u}$ is the fluid velocity and $\varphi$ is the porosity.

Boundary conditions for fluid temperature are supposed to be Dirichlet for the input surface $\Gamma_{f,in}$ and adiabatic anywhere else.

Because of the advection term in equation (3), Galerkin method applied to the weak formulation of (2) and (3) can entail spurious oscillations [8]. To avoid that, a streamline upwind Petrov Galerkin (SUPG) formulation is used, allowing to add numerical diffusion [3, 10].

## 3.3 Radiative transfer

Radiative transfer equation [6] is presented in equation (4) :

$$\vartheta \cdot \nabla I_\nu = -(\kappa_\nu + \sigma_\nu) I_\nu + \kappa_\nu I_{b,\nu} + \frac{\sigma_\nu}{4\pi} \int_{4\pi} p_\nu(\tilde{\vartheta}, \vartheta) I_\nu d\tilde{\vartheta} \tag{4}$$

Where $x$ is the spatial position, $\vartheta$ the direction, $I_\nu$ the intensity, $I_{b,\nu}$ the blackbody intensity, $\kappa_\nu$ the absorption coefficient, $\sigma_\nu$ the scattering coefficient and $p_\nu$ the phase function.

Two discretizations are applied to the radiative transfer equation: angular and spatial. For angular discretization, discrete ordinates method is used on an icosahedron mesh, which can be refined recursively. A system of semi-discrete equations, each with an advection term, is also obtained. As for the hydraulic convection, SUPG method is used for spatial discretization [9, 10]. Basis function $\varphi$ of Galerkin weak formulation are replaced by $\varphi + \delta\vartheta \cdot \nabla\varphi$ for Petrov-Galerkin weak formulation, where $\delta$ is a coefficient function of the mesh size.

A linear system is then solved. Inversion of this system allows to get the intensity field over the semi-transparent domain, and also the energy that is absorbed in.

Materials that are used here are semi-transparent for main wavelengths of solar radiations, but opaque for higher wavelengths, as those of the ambient radiation. In particular, blackbody emission at ambient temperature for main wavelengths of solar radiation are negligible, respect to solar radiation. Source terms can also be computed for a unit solar heat flux, independently of the temperature field.

### 3.4 Numerical coupling

These three finite element models are coupled in order to compute the evolution of the temperature field over the whole structure by knowing the climatic conditions. At each time step, knowledge of solar radiation and temperature field allow to compute, from the linear system of radiative transfer equation, the intensity and then the energy absorbed in the semi-transparent media. Heat and hydraulic convection are then solved by taking into account the thermal heat source induced by solar radiation. A Crank-Nicolson scheme allows finally to compute the temperature field at the next time step [10, 11].

## 4. ENERGY HARVESTING PERFORMANCES EVALUATION

In this section, we first present an overview of thermal performances of solar hybrid roads for some locations in France. From annual weather database, we calculate the temperature field distribution with time and also the output fluid temperature. The energy harvesting is calculated from the fluid temperature rise between input $T_{f,in}$ and output $T_{f,out}$:

$$E = \int_t \rho_f C_{p,f} u S \left(T_{f,out} - T_{f,in}\right)^+ dt \tag{5}$$

Where $S$ is the section of the flow, $u = 1 \times 10^{-4}$m.s$^{-1}$ is the Darcy velocity and $(\cdot)^+$ refers to the positive part.

We consider a length of flow equal to 4 m. The studied period for energy harvesting comes from May to October. In fact, because of thermal inertia, this is the period when the temperature of the structure is the higher during the year in France. Results for energy harvesting are presented in table 3.

**Table 3** Results for energy harvesting

| Location | total solar irradiation [kWh/m$^2$] | $E$ (opaque) [kWh/m$^2$] | $\eta$ (opaque) [%] | $E$(ST) [kWh/m$^2$] | $\eta$(ST) [%] | $\delta E$ [kWh/m$^2$] | $\delta\eta$ [%] |
|---|---|---|---|---|---|---|---|
| Agen | 903 | 339 | 37.5 | 399 | 44.2 | 60 | 6.7 |
| Carpentras | 1034 | 408 | 39.5 | 479 | 46.3 | 71 | 6.8 |
| La Rochelle | 961 | 309 | 32.2 | 381 | 39.6 | 72 | 7.4 |
| Mâcon | 822 | 312 | 38.0 | 367 | 44.7 | 55 | 6.7 |
| Nancy | 786 | 267 | 34.0 | 321 | 40.8 | 54 | 6.8 |
| Nice | 1035 | 424 | 41.0 | 500 | 48.3 | 76 | 7.3 |
| Rennes | 838 | 261 | 31.1 | 320 | 38.2 | 59 | 7.1 |
| Trappes | 833 | 275 | 33.0 | 330 | 39.6 | 55 | 6.6 |

Efficiencies $\eta$ are given as the energy harvest over the cumulated solar irradiation. Subscripts $_{\text{opaque}}$ and $_{\text{ST}}$ refers respectively to the cases of opaque and semi-transparent surface layer. $\delta E$ is the difference between energy harvest of semi-transparent and opaque surface layer and δη is the efficiency increase given respect to the incoming total solar irradiation. Results obtained for the French geographical distribution in energy harvesting and efficiency are shown respectively in figures 3 and 4.

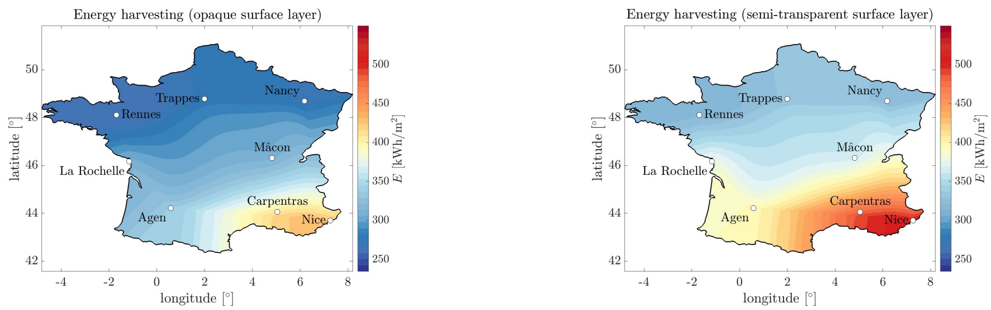


**Fig. 3** Energy harvesting for opaque and semi-transparent surface layer

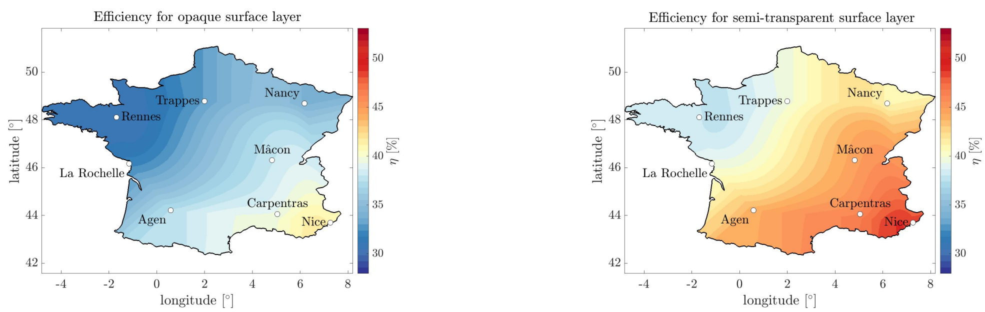


**Fig. 4** Efficiencies for opaque and semi-transparent surface layer

For all these locations, a non negligible part of solar radiation can be recovered, this part being more important when solar radiation and/or average temperature are higher. Using a semi-transparent surface layer allows to obtain an increase in energy harvest between 54 and 76 kWh.m$^{-2}$ for studied locations, corresponding to an efficiency increase of about 7 % by reference to the incident radiation. However, it should be noticed that the energy which is recovered per square meter decreases with the length of the unidirectional porous exchanger. To illustrate that, we present the efficiency distribution as a function of length for Agen in figure 5.

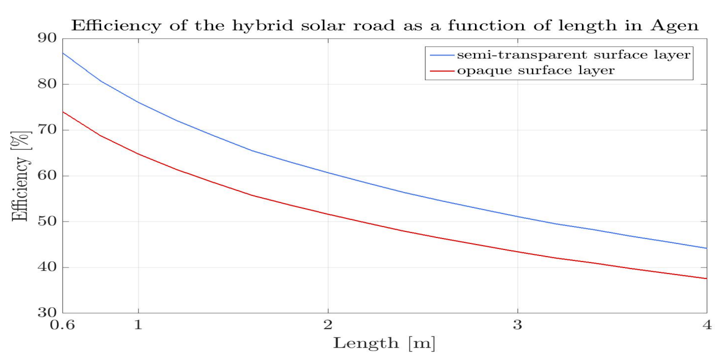


**Fig. 5** Efficiency as a function of length in Agen

In a second step, our model was applied to weather data from Naples (Italy), Montreal (Canada) and Bergen (Norway). In Naples, where mean weather data are closed to Nice, the efficiency increases from 41.5 % with opaque surface layer to 48.3 % with semi-transparent surface layer. In Montreal, where the mean temperature is lower than in France while solar irradiance is closed to Agen, efficiency is lower, with respectively 29.0 and 35.9 %. In Bergen, both mean temperature and irradiance are lower than in France, entailing low efficiencies, equal to 17.6 and 23.2 %. It confirms results and trends observed at France level.

## 5. CONCLUSION

In this paper, we have presented a concept of solar hybrid road and its multi-physics finite element model to solve the coupling between heat diffusion, hydraulic convection and radiative transfer. This numerical model was used to calculate the thermal behavior of such structure in different weather conditions. Energy harvesting in different locations in France is presented and results shows that a non negligible amount of solar energy can be recovered. Using a modified semi-transparent surface layer allows to increase the average energy harvesting of round 7 % by reference to the average solar irradiance in France. In future works a command law to control the surface temperature by acting on the input fluid temperature will be studied. Finally, an improvement of our model would be to take into account surface precipitations in the boundaries conditions.

## REFERENCES

[1] Asfour, S., Bernardin, F., Toussaint, E., and Piau, J.-M., "Hydrothermal modeling of porous pavement for its defreezing," *Applied Thermal Engineering*, 107, pp. 493–500, (2016).

[2] Bejan, A., Dincer, I., Lorente, S., Miguel, A. F., and Reis, A. H., *Porous and Complex Flow Structures in Modern Technologies*, Springer-Verlag, (2004).

[3] Brooks, A. N. and Hughes, T. J. R., "Streamline Upwind/Petrov-Galerkin Formulations for convection dominated flows with particular emphasis on the incompressible Navier-Stokes Equations," *Computer Methods in Applied Mechanics and Engineering*, 32, pp. 199–259, (1982).

[4] Gartling, D. K. and Reddy, J. N., *The Finite Element Method in Heat Transfer and Fluid Dynamics, third edition*, CRC Press, (2010).

[5] Hasebe, M., Kamikawa, Y., and Meiarashi, S., "Thermoelectric generators using solar thermal energy in heated road pavement," *2006 International Conference on thermoelectrics*, IEEE, (2006).

[6] Howell, J., Siegel, R., and Pinar, M., *Thermal radiation heat transfer*, 5th Edition, CRC Press, (2010).

[7] Incropera, F. P. and DeWitt, D. P., *Fundamentals of Heat and Mass Transfer, 5th edition*, CRC Press, (1990).

[8] Johnson, C., *Numerical solutions of partial differential equations by the finite element method*, Cambridge University Press, Cambridge, (1987).

[9] Kanschat, G., (2009). "Solution of radiative transfer problems with finite elements," , *Numerical methods in multidimensional radiative transfer*. Kanschat, G., Meinkhn, E., Rannacher, R., and Wehrse, R. (Eds.). Springer-Verlag Berlin Heidelberg.

[10] LeTouz, N., Dumoulin, J., and Piau, J.-M., "Etude numerique de la resolution du couplage convection/radiation/diffusion dans une structure de chaussée hybride," *Proceedings of Congrès français de thermique 2017*, (2017).

[11] LeTouz, N., Toullier, T., and Dumoulin, J., "Infrared thermography applied to the study of heated and solar pavements: from numerical modeling to small scale laboratory experiments," *Proceedings of SPIE*, (2017). URL `http://dx.doi.org/10.1117/12.2262778`

[12] Liu, X., Rees, S. J., and Spitler, J. D., "Modelling snow melting on heated pavement surfaces, part i: model development," *Applied Thermal Engineering*, 27, pp. 1115–1124, (2007).

[13] Mallick, R. B., Chen, B., and Bhowmick, S., "Harvesting energy from asphalt pavements and reducing the heat island effect," *International Journal of Sustainable Energeering*, 2(3), pp. 214–228, (2009).

[14] Nield, D. A. and Bejan, A., *Convection in porous media, 4th edition*, Springer, (2013).

[15] Ping, T. H. and Lallemand, M., "Transient radiative-conductive heat transfer in flat glasses submitted to temperature, flux and mixed boundary conditions," *Int. J. of Heat Mass Transfer*, 32(5), pp. 795–810, (1989).

[16] Taine, J., Enguehard, F., and Iacona, E., *Transferts thermiques, introduction aux transferts d'nergie, 5th edition*, Dunod, (2014).